

2D Shape Decomposition Based on Combined Skeleton-Boundary Features

JingTing Zeng, Rolf Lakaemper, XingWei Yang, Xin Li

Temple University, Philadelphia, PA
{*jingting.zeng, lakamper, xingwei, xin.li*}@temple.edu

Abstract. Decomposing a shape into meaningful components plays a strong role in shape-related applications. In this paper, we combine properties of skeleton and boundary to implement a general shape decomposition approach. It is motivated by recent studies in visual human perception discussing the importance of certain shape boundary features as well as features of the shape area; it utilizes certain properties of the shape skeleton combined with boundary features to determine protrusion strength. Experiments yield results similar to those from human subjects on abstract shape data. Also, experiments of different data sets prove the robustness of the combined skeleton-boundary approach.

1 Introduction

Shape decomposition is in general defined as complete partition of a single, connected region (shape) into disjunct sets of connected regions (parts). In this scheme, complex shapes are decomposed into simpler components. The task is motivated by results of cognitive research, suggesting that the human visual system uses a part-based representation to analyze and interpret the shapes of objects [1][2][3]. Partitioning schemes are useful in shape matching, shape analysis and many other applications [4][5][6][7].

A recent study on human perception [8] demonstrated that curvature properties of the boundary and the area properties of the enclosed regions affect the observers' identification of contour segments. Similar to previous results from Siddiqi and Kimia [9], their experiments showed that negative minima of contour curvature depict segment boundaries. Additionally segment identification was determined by contour length, the turning angle at part boundaries and the width at the part's base. Motivated by these results, the proposed approach mimics the procedures of human perception assumed in [8] by combining concepts of skeleton and boundary in shape analysis. Our method shows that 'junction points' of the skeleton can provide the possibility of important protrusions. Boundary information as mentioned in [8], including contour length, the turning angle at part boundaries and the width at the part's base, can determine the probability of important protrusions. The proposed decomposition is then based on a definition of protrusion strength, based on both curvature of boundary points and their structural correspondence.

Recently Bai et al. [10] [11] presented robust approaches to compute a perceptually reasonably pruned discrete 2D skeleton of a single boundary. We utilize this skeleton approach. It establishes a correspondence between structural information and boundary

points. Due to its robustness, we use this skeleton approach. Of course any skeleton algorithm offering ‘junction points’ is applicable.

In the following sections, it will be seen that ‘junction points’ of the skeleton play a crucial role in finding a correct decomposition. The motivational connection between junction points and protrusions is the observation that a junction point emanates from the merging of two protrusions. Hence, if the junction points are known, the positions of protrusions can be predicted and the protrusions can be classified as parts or non-parts based on their strength.

The main contribution of this paper is the combination of skeleton and boundary information to simulate human perception based on results of research in visual perception. The experiments directly compare our algorithm with experiments on human subjects. They show that the proposed approach meets the human perceptual intuition. In comparison to classical decomposition methods, our method gives a perceptually more reasonable and stable result. Furthermore, the noisy shape decomposition demonstrates the robustness of our method.

2 Related Work

Shape decomposition is a thoroughly studied field. It mainly splits into two classes of approaches: boundary and region based. In their seminal paper on shape decomposition, Kimia et al. [9] used the boundary curvature to find ‘limbs’ and symmetry axes to find the ‘necks’: the two different features are therefore detected on *separated* examination of boundary and area in contrast to our ‘protrusion’ feature.

Closer to the proposed approach is the decomposition by Mi et al. [12] that combines the smoothed local symmetries and the transition region knowledge to separate parts. However, their computation is based on boundary curve and symmetry axes, which makes it especially hard to detect the compactness of a segment in certain cases. See fig.1 (taken from [12]) for example: the branch (region 1) is inappropriately separated into two parts, since neither the boundary nor the symmetry axes offered sufficient structural information. In contrast, our method preserves the shapes’ structure due to the utilization of skeleton processing (please compare fig.1 to fig.6, right in row 2 and 3).

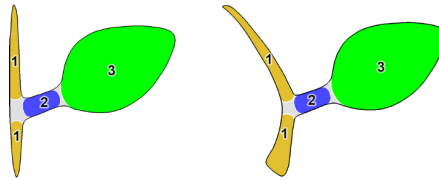


Fig. 1. Examples from [12]. The regions marking as 1 fail to be connected and are separated into two parts individually.

There are other approaches using solely the skeleton information for decomposition: [13] uses the curve skeleton including junction points and user-input points to

decompose 3D shapes (user interactive decomposition). Tanase et al. [14] use skeletons to simplify boundaries successively to obtain protrusion-cut segments. L. Prasad [15] used Constrained Delaunay Triangulation to extract the skeleton and selected successive ‘strong chords’ for decomposition. In comparison to classical methods, our method yields a perceptually more reasonable and stable result. This is mainly achieved through the crucial junction point information with the important boundary features.

3 Decomposition Based on Combined Boundary-Skeleton Features

The *skeleton* S of a boundary B is the locus of the centers of maximal disks in correspondence to [16]. We use the discrete definition of a skeleton as given in [11]: using 8-neighborhood, a skeleton is a connected, thin point set $S = \{s_1, \dots, s_n\}$ describing a geometric graph embedded in \mathbb{R}^2 .

A shape *boundary* is a vector of points $B = \{b_1, \dots, b_m\}$.

An *endpoint* $E_i \in S$ is a skeleton point having only one neighbor.

A *junction point* $J_k \in S$ is a skeleton point with three or more neighbors.

Given a junction point J_k of a skeleton, there is a set of corresponding boundary points intersecting with the maximal disk centered at J_k . We call these boundary points *tangent points* $t_i \in B$ of the junction J_k .

The shortest path between a pair of endpoints on a skeleton graph is called a *skeleton path* P ([17]). We call a partial path between junction or endpoints a *branch*.

With these definitions, we will now describe our decomposition approach. The goal is to find the *part lines* ([9]), i.e. straight connections between a pair of boundary points entirely inside of the shape boundary, to divide a shape region into two parts.

We first compute the skeleton using the Discrete Skeleton Evolution method as proposed in [11]. This approach first computes the skeleton based on Blum’s medial axis definition. Then iterative skeleton pruning (removing end branches) is performed based on a relevance measure which describes the importance of the respective branch for shape reconstruction. The pruning process ends when only major relevant branches remain. We follow [11] and utilize a single threshold as stop criterion. Our experiments showed that this leads to visually correct skeletons in all examples.

After the pruned skeleton is obtained, we choose ‘relevant’ (high negative curvature) pairs of tangent points as candidates to decompose the shape boundary. Each pair of points defines a protrusion. The visual significance, and therewith the final decision for decomposition, is computed as protrusion strength.

Following [8], our decomposition is guided by the following two rules:

(1) decomposition focuses on the turning angle of the part boundary, where the tangent points have negative minima of curvature.

(2) segment identification performance (i.e. strength of protrusion) is related to the segment length and the width at the part’s base.

For an example please see fig.2: we first look at the green path at the blue junction point. The endpoints of the green branch split the boundary into two half boundaries. Red and yellow points mark tangent points on each half boundary. We consider all pairs consisting of one red and one yellow point as candidate split points, i.e. points

defining a part line. In order to do so, we first follow rule 1 to filter candidate pairs with significant negative curvature. As the two points also need to satisfy the second rule, the importance of part protrusion will be calculated to determine the best cut.

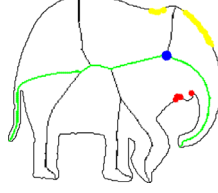


Fig. 2. The junction point in blue has corresponding tangent points of left and right regions shown in red and yellow. We follow the rules to find the pair of tangent points (one from the left region in red and the other from the right region in yellow) to obtain a part line.

Now the process is specified in more detail. Given a path with all its junction points, the task is to determine which of these junction points (if any) define a cut. In the following, we assume to look at the single junction points in order ‘outside to inside’, i.e. starting from both endpoints. The cut-decision process for a single junction point J_k is described as below.

We refer to the two half boundaries defined by the endpoints of the given path as the ‘right’ and ‘left’ boundary (without implication of a preferred direction). For a junction point J_k , the corresponding tangent points on the left boundary are $T^L = \{l_1, \dots, l_p\}$, tangent points on the right boundary are $T^R = \{r_1, \dots, r_q\}$.

With $c(\cdot)$ denoting the curvature in a boundary point (concavities having negative curvature), compute the sum of curvature $C(i, j) = (c(l_i) + c(r_j))$ for all $(l_i, r_j) \in T^L \times T^R$. Also, for each (l_i, r_j) compute the *protrusion strength*, which is defined as follows:

$$P(l_i, r_j, b_k, r) = \frac{|b_k - r|}{|l_i - r_j|} \quad (1)$$

where $|l_i - r_j|$ is the Euclidian distance of l_i and r_j , r is the radius of the maximal disk, see fig.3. b_k is the length of branch with junction point J_k , i.e. the length between J_k and the respective endpoint E . However, if another junction point \hat{J} is between J_k and E , which led to a cut before, b_k is defined as the (shorter) branch length between J_k and \hat{J} .

With a given threshold T , the pair $(l_{\hat{i}}, r_{\hat{j}})$, which minimizes the curvature value, is selected amongst all pairs of points with $P(l_i, r_j, b_k, r) > T$ $C(\hat{i}, \hat{j}) = \min\{C(i, j)\}$. The part line between $(l_{\hat{i}}, r_{\hat{j}})$ defines the split.

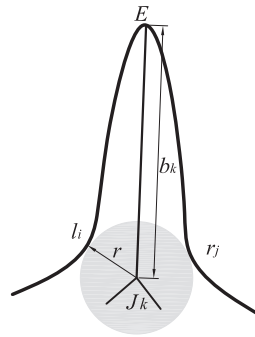


Fig. 3. The computation of protrusion strength.

4 Experiments

4.1 Experiment on Abstract Shapes

For this experiment the shape data from [8] is used to compare our algorithm with performance of human subjects on abstract shapes. In [8], observers were shown an entire shape for a short time and asked to identify the position of a segment in the entire shape. The test was made to prove the hypothesis that segment significance is dependent on protrusion strength. The rationale was “...that identification performance should be superior for contour segments that are more strongly ... emphasized in a shape’s representation” [8]. This means for our experiment, that the strong parts should be among the first to be split in the partitioning process, which is the case as explained below.

Figure 4 gives the original data set with darkened boundary parts for test. The data set has different levels of part significance with respect to the part base line and the elongation: the base width for the test segment increases from top to bottom, the segment length for the test segment increases from left to right. The least significant segment is therefore located in the bottom row, left column.

The result in [8] shows the trend that it was harder for observers to identify the segments of shapes shown at the bottom and left side compared to those at the top and right side of figure 4. For example, only about 40–50 percent of the observers identified the defined segment in (row/column) 3,1 and 4,1 as ‘significant’.

Figure 5 depicts the parts of strongest protrusion resulting from our segmentation. It shows a significant similarity to figure 4: the parts being detected as ‘strong’ parts in our system are those more easily detected in 4. If a segment is significant enough, it is likely to be decomposed as a part and the remaining forms another part (shown in row 1). In some cases our decomposition detects additional parts of comparable protrusion strength, e.g. the first two shapes in row 2. Perceptually, these are comparable to the tested parts. In the case of weak parts (fig. 5, (row/column) 3,1 and 4,1), the parts can not be detected. Hence the entire result follows the trend mentioned above.

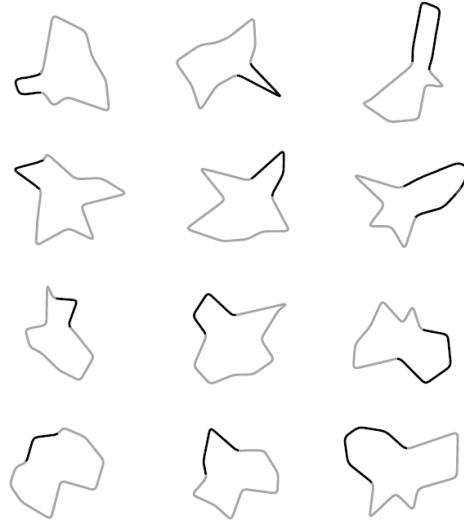


Fig. 4. Data set from [8]. The darkened boundary sections are the test segments of significance.

4.2 Experiment on Different Shapes

This experiment shows decompositions of different shapes, taken from [9], [12] and [15]. Figure 6 shows some results of the proposed algorithm. The consistent decomposition of the object in column 3 is especially remarkable, although heavily distorted by noise. Please compare the improved result on the leaf (right in row 2 and 3) to figure 1.

Figure 7 is a comparison between our method with other decomposition methods, including Kimia’s result [9] and Prasad’s result [15].

4.3 Robustness to Noise

In this experiment, noise was added to data extracted from [18] to show the robustness of the decomposition method. Figure 8 presents 4 groups of shapes, each containing a basic shape in different poses. These poses show non-rigid deformations. Since the approach is based on robust skeleton detection and important boundary features, the decomposition result is consistent. Figure 9 gives the decomposition result for two shapes with evolved noise. It indicates that the increasing noise does not influence the partitioning result.

5 Conclusion and Future Work

We derived a new measure for shape decomposition. Combination of features of pruned skeletons and shape-boundary leads to decomposition results in accord with studies on human perception. The experiments also show the robustness compared to other methods. For future work, we will expand the system to decomposition of 3D shapes.

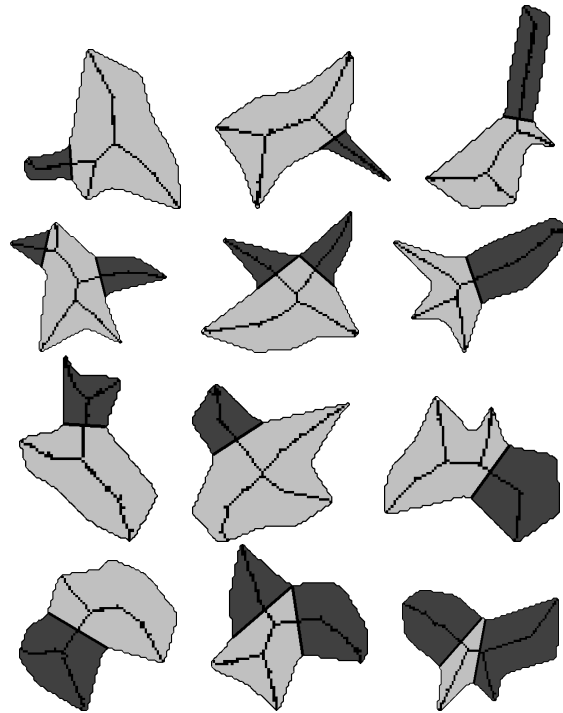


Fig. 5. Decomposition gained by our approach. The results is in accord with the experiment in [8].

6 Acknowledgments

We thank X. Bai and L. Latecki for the skeleton and curvature code, and we also thank the authors of [8], E. H. Cohen and M. Singh for the data set in the first experiment.

References

1. Hoffman, D.D., Richards, W.: Parts of recognition. *Cognition* **18** (1984) 65–96
2. Latecki, L., Lakaemper, R.: Convexity rule for shape decomposition based on discrete contour evolution. *Computer Vision and Image Understanding* **73** (1999) 441–454
3. Singh, M., Hoffman, D.D.: Part-based representations of visual shape and implications for visual cognition. In Shipley, T., Kellman, P., eds.: *From fragments to objects: Segmentation and Grouping in Vision*. Volume 130. (2001) 401–459
4. Puff, D.T., Ebefy, Z.D., Pizerzx, S.M.: Object-based interpolation via cores. In: *Proceedings of SPIE*. (1994) 143–150
5. Abe, K., Arcelli, C., Hisajima, T., Ibaraki, T.: Parts of planar shapes. *Pattern Recognition* **29** (1996) 1703–1711
6. Hilaga, M., Shinagawa, Y., Kohmura, T., Kunii: Topology matching for fully automatic similarity estimation of 3d shapes. In: *Proceedings of the 28th Annual Conference on Computer Graphics and Interactive Techniques*. (2001) 203–212

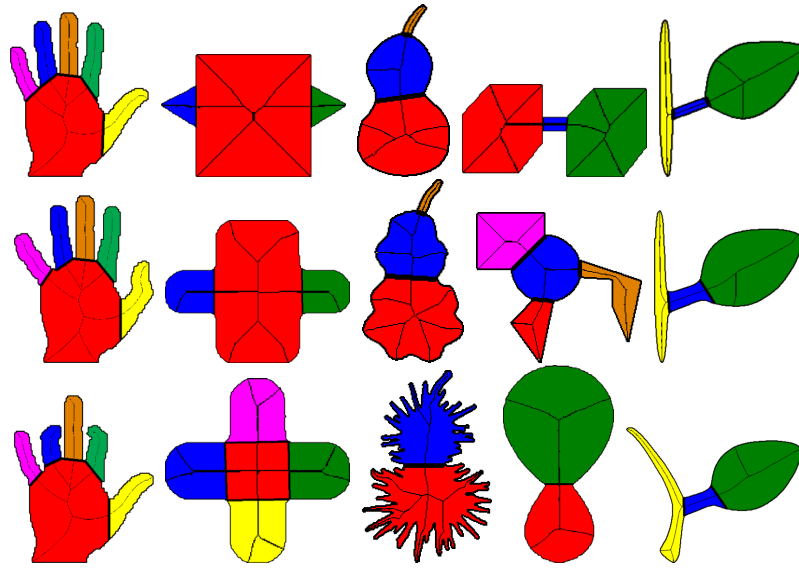


Fig. 6. Decomposition results of our approach on different shapes.

7. Shokoufandeh, A., Bretzner, L., Macrini, D., M.F. Demirci, a.C.J., Dickinson, S.: The representation and matching of categorical shape. *Computer Vision and Image Understanding* **103** (2006) 139–154
8. Cohen, E.H., Singh, M.: Geometric determinants of shape segmentation: Tests using segment identification. *Vision Research* **47** (2007) 2825–2840
9. Siddiqi, K., Kimia, B.B.: Parts of visual form: Computational aspects. *IEEE Transactions on Pattern Analysis and Machine Intelligence* **17** (1995) 239–251
10. Bai, X., Latecki, L.J., Liu, W.: Skeleton pruning by contour partitioning with discrete curve evolution. *IEEE Transactions on Pattern Analysis and Machine Intelligence* **29** (2007) 449–462
11. Bai, X., Latecki, L.J.: Discrete skeleton evolution. In: the 6th International Conference on Energy Minimization Methods in Computer Vision and Pattern Recognition. Volume 4679. (2007) 362–374
12. Mi, X., DeCarlo, D.: Separating parts from 2d shapes using reliability. In: IEEE 11th International Conference on Computer Vision. (2007) 1–8
13. Reniers, D., Telea, A.: Skeleton-based hierarchical shape segmentation. In: Proceedings of the IEEE International Conference on Shape Modeling and Applications. (2007) 179–188
14. Tanase, M., Veltkamp, R.C.: Polygon decomposition based on the straight line skeleton. In: Proceedings of the 19th annual symposium on Computational geometry. (2003) 58–67
15. Prasad, L.: Rectification of the chordal axis transform and a new criterion for shape decomposition. In: Proceedings of the 12th International Conference on Discrete Geometry for Computer Imagery. Volume 3429 of Lecture Notes in Computer Science. (2005) 263–275
16. Blum, H.: Biological shape and visual science. *Journal of Theoretical Biology* **38** (1973) 205–287
17. Bai, X., Latecki, L.: Path similarity skeleton graph matching. *IEEE Transactions on Pattern Analysis and Machine Intelligence* **30** (2008)

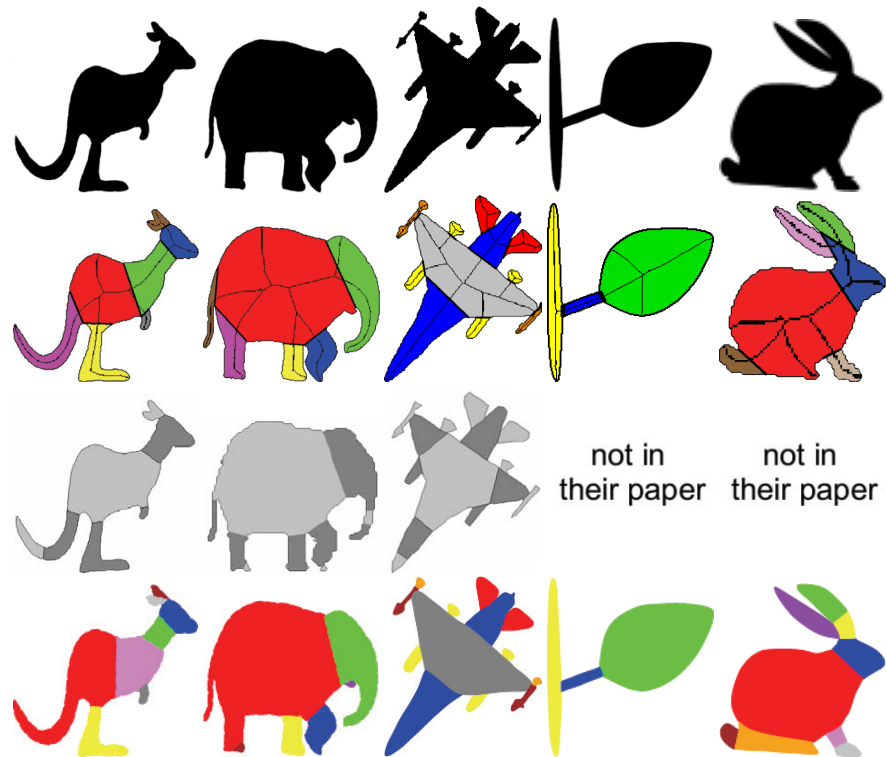


Fig. 7. Results comparison. The first row has five shapes from [9]. The second row shows the results of our algorithm. The third row demonstrates the Prasad's CDT decomposition result [15]. The last row is the results of neck-based and limbed-based method [9].

18. Baseski, E., Erdem, A., Tari, S.: Dissimilarity between two skeletal trees in a context. *Pattern Recognition* (2008)

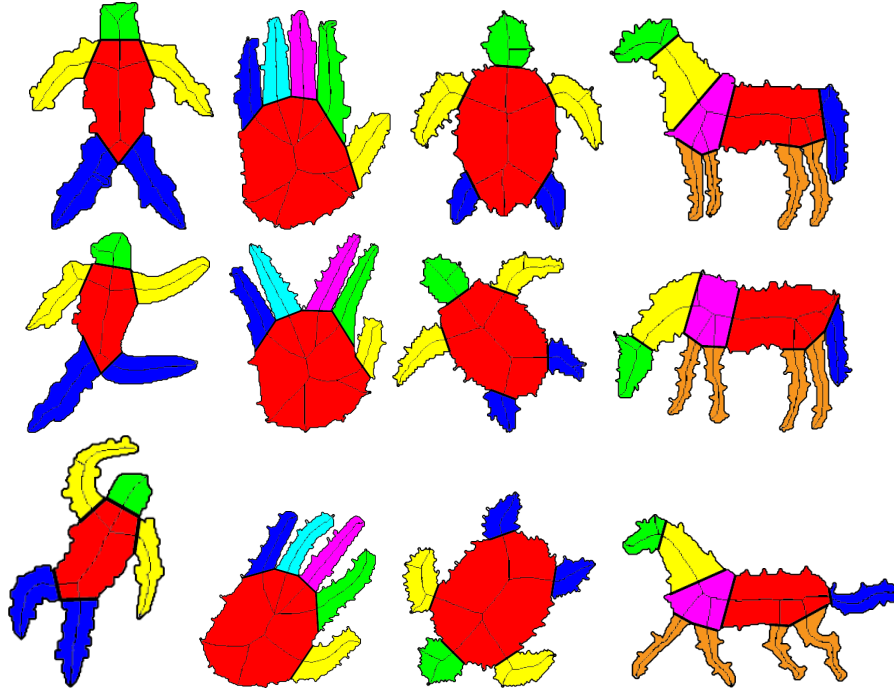


Fig. 8. The decomposition result of noisy shapes.

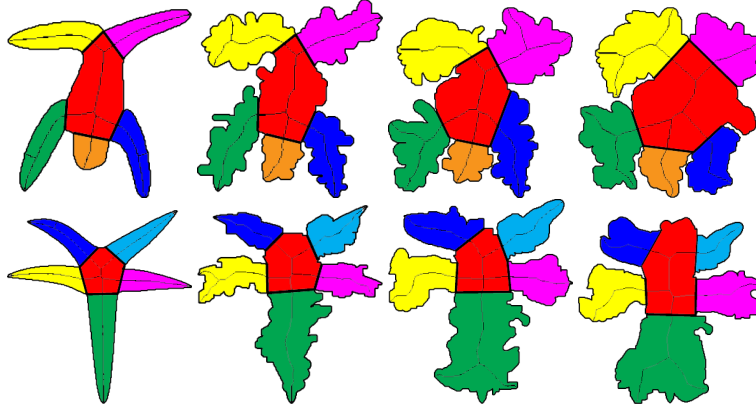


Fig. 9. The decomposition result of two noisy shapes. the first column shows the original shapes. Columns 2,3 and 4 add 5%, 10% and 15% of noise respectively, where noise rate is based on region-difference.